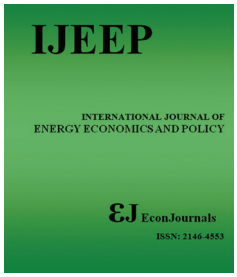

International Journal of Energy Economics and Policy

ISSN: 2146-4553

available at http: www.econjournals.com

International Journal of Energy Economics and Policy, 2026, 16(2), 714-729.

Advanced Time Series Forecasting of Electricity Generation in Turkey: A Comparative Study Using LSTM Models, ARIMA, and PSO - Optimized Holt Trend

Menşure Zühal Barak*, Esra Karakaş

Department of Business Administration, Faculty of Economics, Administrative and Social Sciences, Adana Science and Technology University, Adana, Turkiye. *Email: mzbarak@atu.edu.tr

Received: 25 August 2025 **Accepted:** 19 December 2025 **DOI:** https://doi.org/10.32479/ijeep.22153

ABSTRACT

This study examines energy production forecasting in Turkey through advanced time series methodologies. The analysis, conducted on annual data spanning the period 1970-2024, encompassed not only aggregate electricity generation but also disaggregated production from coal, natural gas, hydro, and renewable sources, including waste. The modeling framework integrated both conventional and machine learning-based techniques, specifically ARIMA, single-layer and three-layer LSTM architectures, and Holt's linear method optimized via particle swarm optimization (PSO). Model performance was assessed using widely recognized error metrics, namely mean absolute percentage error (MAPE), mean squared error (MSE), and root mean squared error (RMSE). The empirical results demonstrated that the three-layer LSTM model achieved the lowest error values for total, coal, and hydro-based generation, whereas the single-layer LSTM exhibited superior accuracy for natural gas. In contrast, the traditional ARIMA model yielded the most precise forecasts for renewable and waste-based energy. These outcomes underscore that while deep learning models such as LSTM are capable of capturing intricate temporal dynamics when appropriately tuned, conventional models like ARIMA continue to demonstrate robust predictive capability for specific datasets. Overall, the findings confirm that all four approaches provide an acceptable level of forecasting accuracy.

Keywords: Turkey Electric Production Forecast, Long Short-Term Memory, Autoregressive Integrated Moving Average, Holt Method, Particle Swarm Optimization, Time Series Forecasting
JEL Classifications: Q47, C45, C53, C61

1. INTRODUCTION

Electricity production is a key driver of economic growth, energy security, and environmental sustainability. For rapidly developing countries like Turkey, expanding investments in electricity generation is essential to meet rising energy demands while fulfilling ecological commitments. As the electricity generation sector plays a central role in achieving net-zero carbon targets, it is critical to support the investment toward sustainable, reliable, and efficient energy systems (Ren et al., 2024). Furthermore, prioritizing renewable and environmentally friendly energy technologies not only enhances economic resilience but also preserves environmental integrity.

Turkey's growing population and expanding economy have accelerated electricity demand, making strategic generation planning a priority to support economic development. Electricity production is not only a fundamental production factor but also crucial for energy security and environmental sustainability (Lucia and Grisolia, 2017). Increasing global warming and ecological pollution pressures have further emphasized the importance of renewable energy investments. The long-term relationship between renewable energy production and economic performance highlights the decisive role of energy efficiency in national development (Inglesi-Lotz, 2016). In economies where fossil fuels remain dominant, such as Turkey, implementing renewable energy technologies is indispensable for meeting growing energy

demand while mitigating environmental pollution (Paul and Uhomoibhi, 2012).

Countries with high solar irradiation, like Turkey, benefit from promoting renewable energy to enhance energy security, generate employment, and support sustainable growth. However, the intermittent nature of renewable sources such as solar and wind causes variability that can challenge grid stability and reliability, making accurate electricity production forecasting essential (Notton et al., 2018). Accurate forecasting enables improved planning and management, reducing energy losses and enhancing operational efficiency (Voloshko et al., 2019). Governments investing in forecasting capabilities can more effectively meet rising energy demand while adhering to global emission reduction commitments (Owusu and Asumadu-Sarkodie, 2016).

Forecasting electricity production in Turkey is critical due to the need for sustainable development policies, effective management of rising energy demand, and integration of renewable energy into the grid (Yılmaz, 2023). Increasing electricity demand, combined with insufficient installed capacity, creates a significant supply-demand imbalance, which poses economic, environmental, and strategic risks, especially for a country dependent on energy imports (Kıran et al., 2012). Accurate forecasts are essential for energy policy and capacity planning, supporting transitions to renewable energy, reducing greenhouse gas emissions, and enhancing energy independence (Kurt et al., 2022). Due to limited electricity storage, production must match consumption, requiring precise forecasting models to minimize economic losses from over- or under-production (Oscar, 2021).

In light of the increasing importance of reliable energy forecasting for policy and planning, this study aims to develop a comprehensive modeling framework for Turkey's electricity generation covering the period 1970-2024. The analysis incorporates both aggregate electricity production and disaggregated outputs from coal, natural gas, hydro, and renewable and waste sources. To this end, a comparative approach is employed that combines traditional time series techniques (ARIMA), machine learning methods (single- and three-layer LSTM), and an optimization-based exponential smoothing model (Holt's linear method optimized with Particle Swarm Optimization). By evaluating the models through multiple performance metrics (MAPE, MSE, RMSE), the study seeks to identify the most effective forecasting strategies for different energy sources. The findings contribute to the literature by demonstrating the complementary strengths of classical and deep learning-based approaches in capturing the dynamics of Turkey's energy sector. Moreover, this comprehensive approach aims to generate more reliable and robust forecasts, which are essential for ensuring energy supply security and accelerating the transition toward renewable resources.

2. LITERATURE REVIEW

The increasing importance of electrical energy has led to a corresponding rise in studies concerning the Turkish electricity sector. The existing literature contains numerous forecasting models that analyze critical factors such as demand predictions, future scenarios for renewable energy production, and the impact of pricing and policy. A review of previous work reveals a recent surge in studies that employ machine learning and artificial intelligence methods, driven by the growing complexity of electricity generation and consumption, the inherent difficulties of forecasting within the electricity market, and the diversification of statistical, machine learning, and AI methodologies developed to address these challenges. Another fundamental reason for this increase is the ever-growing significance of electrical energy, which is critical for national security and aligns with countries' social and economic development strategies. Accurate forecasting of electricity production is paramount, as energy storage is a complex and costly process.

The literature on energy production forecasting in Türkiye is characterized by a blend of statistical, computational, and economic methods aimed at understanding and predicting the country's energy demand dynamics. Various studies have utilized advanced forecasting techniques to provide insights into electricity production trends within Türkiye's rapidly evolving energy landscape.

Among traditional statistical methods, Haliloğlu and Tutu (2018) successfully employed the SARIMA (seasonal autoregressive ıntegrated moving average) model to forecast daily electricity demand in Türkiye, achieving a remarkably low error rate of approximately 1% (Haliloğlu and Tutu, 2018). Other studies have combined seasonal analysis with Artificial Neural Networks (ANN) to forecast monthly sectoral electricity consumption. Akay and Atak (2007) developed a model using the Grey Prediction method, integrated with a rolling mechanism, to forecast total and industrial electricity consumption (Akay and Atak, 2007). Hamzaçebi (2007) applied ANNs for sectoral net consumption forecasting and noted their high success rate with non-linear data, highlighting their suitability for such tasks (Hamzaçebi, 2007). Similarly, the Seasonal ANN model, explored by Hamzaçebi et al. (2019), was found to be highly accurate for monthly predictions (Hamzaçebi et al., 2019). Using data from 1986 to 2013 for 21 regional distribution companies in Turkey, the study employs ARIMA-based time series, panel, and spatial panel data models to forecast electricity demand, finding that the pooled panel model provides the best performance according to RMSE and highlighting the importance of regional interactions and spatial dependencies in energy planning and policy (Akarsu, 2017).

Acar et al. (2021) utilized Seasonal ARIMA for monthly forecasts, providing a critical solution for mid-term planning (Acar et al., 2021). In his 2016 study, Günay used an ANN model with socio-economic and climatic variables as inputs to predict that Türkiye's annual total electricity demand would double by 2028 (Günay, 2016). Kankal and Uzlu (2017) demonstrated that an ANN model enhanced with the Teaching-Learning-Based Optimization (TLBO) algorithm significantly outperformed other ANN structures by reducing error rates. This work provided an effective method for long-term electricity demand forecasting using historical consumption data and socio-economic indicators (Kankal and Uzlu, 2017). More recently, Saglam et al. (2023) used Medium-Scale Neural Networks (MNN) to forecast Türkiye's

electricity needs up to 2040 (Saglam et al., 2023). Other advanced techniques include the hybrid model developed by Kaytez (2020), which combined ARIMA and least squares support vector machine (LSSVM) methods for net electricity consumption forecasting (Kaytez, 2020). Additionally, specific studies, such as the one by Özbay and Dalcalı (2021), have focused on unique periods like the COVID-19 pandemic, where they developed an ANN model for short-term forecasting of electricity consumption in Türkiye (Özbay and Dalcali, 2021).

One of the most significant and increasingly important areas of research is forecasting for renewable energy production. Utkucan Şahin (2020) developed an advanced fractional nonlinear grey bernoulli model (FANGBM) to forecast that Türkiye's total renewable installed capacity and electricity production will continue to increase significantly until 2030, though the share of hydropower is expected to decline (Şahin, 2020). Soğukpınar et al. (2023) examined the impact of renewable energy policies on the entire energy system, revealing that an increase in renewable installed capacity has a significant negative effect on long-term sectoral electricity demand (Soğukpınar et al., 2023). This suggests that renewable energy policies promote efficiency and reduce overall consumption, thereby contributing to economic and environmental sustainability. Other specialized studies on renewable energy include Yıldızhan and Sivrioğlu (2015) and Yüzer (2023), who investigated the future of solar energy capacity (Yildizhan and Sivrioğlu, 2015). Ertekin (2020) proposed an hour-based ensemble machine learning method for solar power prediction, which is crucial for grid integration (Ertekin, 2020).

In terms of forecasting studies on emissions, pricing, and economic impact, Bakay and Ağbulut (2021) used deep learning, support vector machines, and ANN algorithms to predict greenhouse gas emissions from electricity production, finding that CO_2 constitutes the largest share (Bakay and Ağbulut, 2021). On the market side, Ugurlu et al. (2018) found that the SARIMA model was the most effective for forecasting hourly prices in Türkiye's Day-Ahead Electricity Market (Ugurlu et al., 2018). The broader economic interaction was explored by Akdağ and Ekici (2022), who analyzed the impact of energy production and consumption on Türkiye's industrial index (Akdağ and Ekici, 2022).

Current research continues to push the boundaries of forecasting accuracy and application areas, with a growing focus on advanced neural network studies. Bulut (2024) utilized long short-term memory (LSTM) for both consumption and production forecasting related to hydroelectric power (Bulut, 2024). Bişkin and Çifci (2021) also employed LSTM, as well as more advanced deep learning models like gated recurrent unit (GRU) networks (Bişkin and Çifçi, 2021). Moreover, Bulut (2024) and others are increasingly focusing on multi-feature production sources, such as assessing the potential for energy recovery from wastewater treatment plants.

The body of work on electricity production and consumption forecasting in Türkiye is comprehensive and encompasses a wide range of methodologies. These studies demonstrate a clear evolution from traditional statistical methods to highly sophisticated artificial intelligence and machine learning models, which consistently provide superior accuracy by capturing the complex, non-linear dynamics of the energy system. Previous research has addressed a broad spectrum of needs, ranging from long-term, strategic forecasts that guide infrastructure investment and national energy policy to short-term, high-frequency predictions essential for daily grid stability and economic operation.

3. MATERIALS AND METHODS

Due to the inherently nonlinear and dynamic characteristics of electricity generation data, the selection of forecasting methods becomes a critical issue. When choosing an appropriate method, factors such as the statistical structure of the data, the amount of data available, the interpretability of the model, and the forecasting horizon are taken into consideration. While traditional models such as ARIMA or the Holt model can provide satisfactory results for simple and short-term series, deep learning-based approaches tend to perform better in cases that involve complex structures or require long-term forecasts. Traditional methods often fall short in capturing the complex dynamics of the data, whereas approaches such as long short-term memory (LSTM) networks can achieve higher accuracy (Zhang and Li, 2022)

In this regard, in this study, it was aimed to forecast Turkey's electricity generation sources until 2030 but also to compare the performance of different method, ARIMA, Holt's linear method optimized with particle swarm optimization (PSO), and single and multi-layer LSTM models in order to reveal which approaches are more effective in handling varying data structures. By combining classical statistical techniques with advanced machine learning models, the study provided a comprehensive framework that justifies the selection of these methods for analyzing Turkey's electricity production dynamics.

3.1. Materials

In this study, annual data spanning the years 1970-2024 was used to forecast Turkey's long-term electricity production potential. The accuracy and reliability of the data were of critical importance for the validity of the study's findings. For this reason, the data was compiled from two main reliable sources:

- Annual electricity production data for the years 1970-2023 was obtained from the official database of the Turkish Statistical Institute (Institute, 2025)
- The data for the year 2024 was obtained from the public sources of the Turkish Republic Ministry of Energy and Natural Resources (Resources, 2025).

The analyzed datasets were classified on an annual basis as electricity production data obtained from the main sources under the headings coal, natural gas, hydroelectric (Hydro), and renewable energy and wastes. Additionally, there was also data on the total electricity production obtained from all these sources on a yearly basis.

Figure 1 illustrated Turkey's annual total electricity generation and its subgroups in GWh over the period 1970-2024. When Figure 1 is examined, it was seen that the overall trend in electricity

Figure 1: Electricity production of Turkey from 1970 to 2024

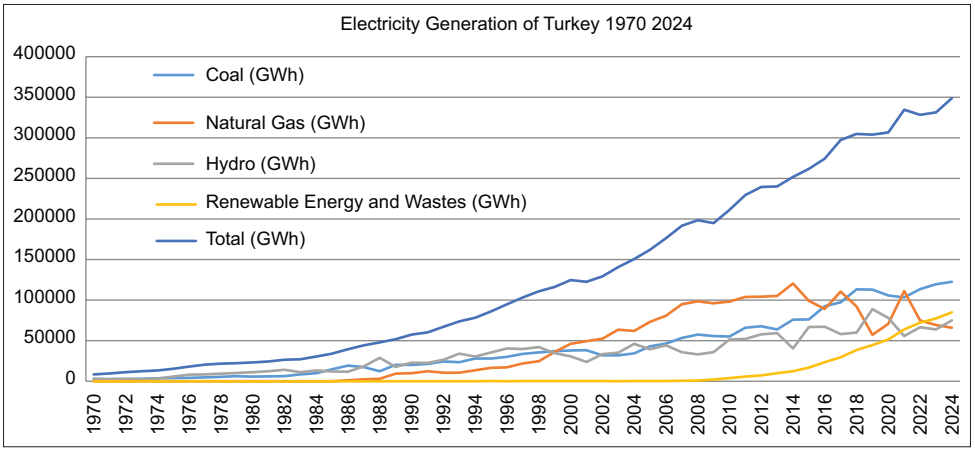

production began with a stable yet relatively moderate increase from the early 1970s to the late 1980s. This growth was most likely shaped by gradual capacity expansions and relatively limited industrial development during that period. From the late 1990s to the mid-2010s, however, Turkey's energy demand rose sharply, increasing nearly six-fold between 1970 and 2010, with electricity demand following a similar trajectory. In 2010, the total installed capacity reached 49,524 MW, generating 211,208 GWh of electricity; this figure was four times the production level recorded in 1990 (Atilgan and Azapagic, 2016). After 2010, the upward trend became even more pronounced, reflecting substantial investments in electricity generation infrastructure as well as diversification of the energy mix. A slight deceleration and fluctuations observed around 2018-2020 can be associated with the impacts of the COVID-19 pandemic on the economy. Overall, from a time series perspective, the dataset exhibits a persistent upward trend with only short-term deviations.

Turkey's annual electricity generation dataset was composed of five main subgroups: Coal, Natural Gas, Liquid Fuels, Hydro (Hydroelectric), and Renewable Energy and Wastes. When Figure 1 was analyzed, it was observed that electricity generation from coal followed an increasing trend throughout the 1970-2024 period, maintaining a significant share in total electricity production. Despite its importance in Turkey's electricity mix, coal is also one of the main sources of greenhouse gas emissions, contributing heavily to air pollution and global climate change. Coal-based electricity generation in Turkey showed a rapid increase until 2020, partly due to COVID-19 and environmental effects, yet it displayed a more moderate upward trend towards 2024.

Another key source of electricity generation for Turkey is natural gas. As Figure 1 indicates, electricity production from natural gas began in 1985. Since it is largely dependent on imports, natural gas generation has shown fluctuations over the years due to policies, pricing strategies, and the effects of external dependency. The highest utilization rates were reached in 2017 and 2022, but following the COVID-19 pandemic, the sharp increase in natural gas-based generation gave way to a more stable pattern.

With its vast geography, mild climate, and rich river basins, Turkey is also one of the countries with significant potential in hydroelectric generation. Electricity production from hydro increased rapidly with the construction of hydroelectric power plants. Nevertheless, hydroelectric output has been highly influenced by natural factors (precipitation and water regime), technical factors (turbine efficiency and maintenance), and environmental-political factors (water management and energy policies). Consequently, hydroelectric generation has stagnated after 2017.

The Renewable Energy and Wastes subgroup refers to electricity generated from renewable sources such as solar, wind, and biomass, as well as from waste incineration plants. In recent years, this category has shown a marked upward trend. While electricity generation from renewables declined and nearly approached zero between 1970 and 1985, it started to rise again after 1985, with a strong acceleration particularly in the last decade. The main drivers behind this growth include increasing environmental awareness, energy diversification policies, technological progress, and international influences.

Finally, Liquid Fuels, which had been used for electricity generation in Turkey since 1970, displayed a steady downward trend and has significantly declined over the last decade. By 2024, liquid fuels were no longer used for electricity generation. Therefore, as it was considered that this category would not provide a meaningful contribution to future forecasting models, the data on liquid fuels was excluded from the analysis.

3.2. Methods

Comparing different forecasting methods is crucial for analyzing the accuracy of their results. In this study, while each data series generally showed an increasing trend, they also exhibited distinct developments over the years. Therefore, it is more appropriate to select a suitable method for each dataset and perform the future forecast using that method.

Studies in the literature reveals that traditional time series models, such as the Box-Jenkins ARIMA method, are among the most widely used. In addition, Holt's method, a type of exponential smoothing, has been shown to be successful with data that has a linear trend but no seasonality, which is the case with the data in this study. Deep learning-based models like

LSTM provide higher accuracy for data that is nonlinear and contains long-term dependencies (Al-hamid and Savaş, 2023). Because accurate analysis of total electricity production and its sub-components was necessary for this study, a forecasting analysis was conducted on all datasets using four different methods, as this is a forecasting problem that requires analysis with multiple approaches. In this study, the Box-Jenkins ARIMA, two different LSTM models, and the Holt linear trend method optimized with PSO were used.

3.2.1. ARIMA model

The development and implementation of ARIMA (autoregressive ıntegrated moving average) models as forecasting tools is commonly referred to as the Box-Jenkins methodology. This approach to time series analysis involves identifying an appropriate ARIMA(p,d,q) model that sufficiently captures the underlying stochastic process generating the observed data. The methodology consists of three fundamental stages: Model identification, parameter estimation and diagnostic checking, followed by forecasting (Dritsakis and Klazoglou, 2018).

The process begins with determining whether the time series is stationary. If the series exhibits non-stationarity, it is transformed through differencing—first-order, second-order, or higher—until stationarity is achieved. The degree of differencing required (d) is determined during this phase, supported by statistical tests for unit roots, such as the Augmented Dickey-Fuller (ADF) test or autocorrelation function (ACF). If autocorrelations start high and decline slowly, then series is nonstationary, and should be differenced (Dobre and Alexandru, 2008)

Once stationarity have been addressed, the next step is to identify the appropriate order of the autoregressive (p) and moving average (p) components. This is typically achieved by analyzing the patterns in the autocorrelation function (ACF) and partial autocorrelation function (PACF) of the series. The sample autocorrelation plot and the sample partial autocorrelation plot are compared to the theoretical behaviour of these plots when the order is known (Hanke and Winchern, 2014:400). After identifying the model, the parameters for the AR terms and the MA terms are estimated. Box-Jenkins models are typically estimated using either the least squares method or maximum likelihood (MLE) method (Dobre and Alexandru, 2008).

The ARIMA model is expressed as the following mathematical formula 1 (Buhan et al., 2022).

$$Z_t = \delta + \phi_1 Z_{t-1} + \phi_2 Z_{t-2} + \cdots + \phi_p Z_{p-1} + \epsilon_t - \theta_1 \epsilon_{t-1} - \theta_2 \epsilon_{t-2} - \ldots - \theta_q \epsilon_{t-q} \quad (1)$$

Where Z_t denotes the forecasted value at the time t and $Z_{t-1},\ldots,Z_{t-p}$ represent the observed values from previous times, with p indicating the order of the AR component of the model. The term δ is a constant that is defined by the AR coefficients. The parameters $\phi_1,\ldots,\phi_p$ are the AR coefficients, while $\theta_1.,\theta_q$, are the MA coefficients. The terms $\epsilon_t,\ldots\epsilon_{t-q}$ correspond to the residuals with q denoting the order of the MA components.

Finally, the diagnostic checking stage involves assessing whether the residuals of the estimated model behave as white noise, confirming that the model adequately captures the structure of the time series. In this case, the residuals should not exhibit autocorrelation. If the model fails diagnostic tests, modifications are made, and the previous steps are repeated to identify a more suitable model (Dritsakis and Klazoglou, 2018).

To assess whether the residuals from the fitted ARIMA model exhibit white noise behavior, the Ljung-Box Q-test is commonly employed. This diagnostic test evaluates whether a group of autocorrelations in the residuals significantly deviates from zero. A low P-value associated with the Q statistic (e.g., $P < 0.05$) suggests that the model fails to adequately capture the underlying structure of the data. In such cases, the analyst should consider specifying a new or modified model and continue the modeling process until a satisfactory fit is achieved (Meyr, 2014).

3.2.2. The lstm (long short-term memory) methods

The LSTM (long short-term memory) method is a specialized type of RNN (recurrent neural network) model. While LSTM networks share a similar architecture with recurrent neural networks, they represent a unique class of artificial neural networks that offer significant advantages. Standard RNNs, which use the output from a previous step as the input for the next, progress in sequential steps and are limited by their short-term memory. This characteristic makes them effective for addressing sequential data problems like natural language processing and time series analysis. However, due to their limitations in learning and retaining long-term dependencies, crucial information can often be lost early in the network's processing.

The LSTM architecture is specifically designed to overcome these challenging loss scenarios found in traditional RNNs. The design of LSTM cells incorporates "gates" that regulate and control the flow of information. Within this structure, the forget gate determines which information within the cell state should be retained or discarded, while the input gate decides how much of the new information will be added to the cell. The cell state is then updated based on these decisions, ensuring that information is stored in long-term memory. Finally, the output gate generates the hidden state (ht) based on the updated cell state, and this state is passed as input to the next step.

The dynamic state of a long short-term memory (LSTM) cell is defined by four fundamental components: The input gate (i_t), the forget gate (f_t), the output gate (o_t), and the cell state (c_t). These gates are formulated using the sigmoid (σ) and hyperbolic tangent (tanh) activation functions, incorporating the previous hidden state (h_{t-1}) and the current input vector (x_t) (Ran et al., 2019). The parameters are represented by the matrices and vectors W and b. These relationships are expressed by the following formulas:

$$i_t = \sigma\,(W_i\, h_{t-1}, x_t\,] + b_i \quad (2)$$

$$c_t = \tanh\,(W_c\,[h_{t-1}, x_t] + b_c) \quad (3)$$

$$f_t = \sigma\,(W_f\,[h_{t-1}, x_t] + b_f) \quad (4)$$

$$c_t = f_t * c_{t-1} + i_t * \tilde{c}_t \quad (5)$$

$$o_t = \sigma\,(W_o\,[h_{t-1}, x_t] + b_o) \quad (6)$$

$$h_t = o_t \odot \tanh(c_t) \quad (7)$$

3.2.3. The PSO optimised Holt linear trend method

The Holt's method, developed by Charles Holt in the 1950s, is a variation of the exponential smoothing method that considers both the level and the trend. This method is particularly effective for time series where the underlying data show a consistent upward or downward movement over time (Holt, 2004). Unlike the ARIMA method, the Holt Linear Trend method does not require the data to be stationary (Tak et al., 2021). Furthermore, the Holt Linear Trend method inplace of Holt Winters method was used in this study because the data were annual, showed an overall increasing trend over the years, and seasonal analysis could not be performed on annual data. The formulas (8), (9), (10) for the forecast, level, and trend for the Holt's linear trend method are as follows:

$$\hat{y}_{t+h\backslash t} = m_t + hx_t \quad (8)$$

$$m_t = \alpha y_t + (1-\alpha)\,(m_{t-1} + z_{t-1}) \quad (9)$$

$$b_t = \beta\,(m_t - m_{t-1}) + (1-\beta)\,(z_{t-1}) \quad (10)$$

The forecast for the series at time *t* is denoted by $\hat{y}_{t+h\backslash t}$. The level of the series at time *t* is represented by m_t, while its trend is b_t. The parameter α is the level smoothing parameter, and β is the trend smoothing parameter, both of which have values between 0 and 1 (Yapar et al., 2018).

Holt's linear trend method uses two smoothing parameters, α (the level coefficient) and β (the trend coefficient). Selecting optimal values for these coefficients is of critical importance, as incorrect choices can lead to issues of overfitting or underfitting. These parameters can take on values between 0 and 1, and the infinite number of possible values makes the solution complex. The fact that there are infinite coefficient possibilities between 0 and 1, and finding which coefficient will yield the best result, is a type of optimization problem. Traditional trial-and-error methods are inefficient, especially with large datasets, which is why automatic optimization techniques are needed (Pangestu and Andayani, 2023). For this reason, modern heuristic methods that provide faster and more accurate results are used today.

The studies in the literature shows that Particle Swarm Optimization (PSO) stands out as an effective meta-heuristic method for optimizing Holt's smoothing parameters. For instance, Hakimah and Kurniawan (2020) combined PSO with the damped trend exponential smoothing method to achieve better results in exchange rate forecasting compared to manual parameter selection (Hakimah and Kurniawan, 2020). Similarly, it was demonstrated significant improvements in construction cost index forecasting by integrating PSO with the Holt-Winters smoothing method (Ebesek and Ebesek, 2023). These findings suggest that PSO offers a distinct advantage over static optimization methods for the dynamic improvement of parameters in time series models. In the context of the Holt linear trend method, PSO minimizes error metrics by exploring different (α, β) combinations.

Particle swarm optimization (PSO) is a computational technique inspired by the social behavior patterns of bird flocks or similar swarms, where individuals (particles) collectively explore the solution space. Candidate solutions are guided towards the best solution in high-dimensional solution spaces by being updated at each step according to their own best position and the swarm's best position (Kennedy and Eberhart, 1995). This mechanism is formulated to be compatible with changes in the velocity and position of birds and is applied to various optimization problems.

Particle swarm optimization (PSO) has been widely used due to its simplicity, efficiency, and broad applicability (Wu et al., 2022). The versatility and simplicity of PSO enable its application across various fields such as engineering optimization problems, machine learning, and economics (Jiang et al., 2020). The inherent parallelism of the algorithm allows for a robust exploration of the solution space, facilitating efficient convergence toward optimal or near-optimal solutions.

The algorithm consists of several iterative steps designed to improve solution accuracy. Considering a particle in an N-dimensional space, let the position vector be defined as $X_i = (x_{i1}, x_{i2}, x_i)$ and the velocity vector as Vi = (vi1, vi2.,viN). Initially, a predefined number of particles are placed within the search space. Unless otherwise constrained, these positions and velocities are assigned randomly. Each particle represents a potential solution to the optimization problem. The initial positions can be determined according to problem constraints, while velocities are generally set as small random values (Matrenin and Sekaev, 2015).

In the fitness evaluation step, each particle's position is assessed using a fitness function, which measures how close the solution is to the optimization objective. The performance of each particle is recorded, and its best position so far is stored in memory as *pBest* (Wu et al., 2022). The local best position of a particle is expressed as $pbest_i = (p_{i1}, p_{i2}, \ldots p_{iN})$. For the global best determination, the algorithm identifies the best position among all particles, known as the *gBest*. This position serves as a guiding reference during the swarm's exploration of the search space. The global best vector is expressed as $gbest_i=(pbest_1, pbest_2, pbest_N)$. Finally, in the velocity update step, each particle's velocity is iteratively updated based on its previous velocity, its distance from pBest, and its distance from gBest. The velocity update of a particle is defined as:

$$V_{i(t)} = w_{(t)}\,V_{i(t-1)} + c_1 r_1\,(X(pbest)_i - X_{i(t-1)}) + c_2 r_2\,(X(gbest)_i - X_{i(t-1)}) \quad (11)$$

After updating the velocity, the position update is performed. Each particle's position is modified using its new velocity, enabling particles to explore new regions of the solution space. The position update of a particle is expressed as:

$$X_{i(t)} = V_{i(t)} + X_{i(t-1)} \quad (12)$$

This equation 12 determines how the position of a particle in the search space changes according to its velocity and direction. Here, ttt denotes the iteration number. Equation ensures that a particle's position in space is updated with its newly calculated velocity. The new velocity is determined based on the particle's previous velocity, its current position, and its distances to both *pBest* and *gBest* (Wu et al., 2022).

In the velocity update formula 11, $w_{(t)}$ represents the inertia weight, which controls how much of the previous velocity is carried into the new velocity. The terms r_1 and r_2 are random numbers uniformly distributed between 0 and 1. The acceleration coefficients are generally set as c1=c2=2, since adopting this value has been shown in the literature to yield effective results. This formulation enables a balance between exploration (searching new areas) and exploitation (refining known promising areas) (Wu et al., 2022). Finally, in the termination phase, the search process is repeated until a stopping criterion is satisfied such as reaching the maximum number of iterations, achieving a satisfactory fitness level, or observing no significant improvement over a certain number of iterations (Wu et al., 2022).

3.2.4. Error evaluation metrics

The mean absolute percentage error (MAPE), mean square error (MSE), and root mean square error (RMSE) are crucial metrics for evaluating the effectiveness of forecasting models. Each of these metrics serves as an indicator of the accuracy and reliability of predictions, guiding researchers in model selection and improvement. The mean absolute percentage error (MAPE) is a scale-independent error metric commonly used to evaluate the performance of forecasting models. It calculates the average of the absolute errors between actual values and forecasts, expressed as a percentage of the actual values. Since MAPE is presented in percentage terms, it is considered one of the most intuitive and easy-to-understand forecasting error measures. Generally, a MAPE value of <10% is regarded as indicating excellent forecasting accuracy, while values between 10% and 20% are considered to represent moderate forecasting accuracy (Chairunnisa and Fauzan, 2023).

The formula for MAPE is expressed as follows:

$$\text{MAPE} = \%100 / n * \sum_{i=1}^{n} \left| \frac{y_i - \tilde{y}_i}{y_i} \right| \quad (13)$$

- y_i: The actual (observed) value at time t,
- $\tilde{y}_i$: The forecasted value at time t,
- n: The number of observations,

The mean squared error (MSE) is a fundamental metric used to quantitatively evaluate the performance of forecasting models by calculating the average of the squared prediction errors. By squaring the errors, MSE places greater emphasis on larger errors compared to smaller ones, thereby encouraging the reduction of large deviations during the model development process. Due to its straightforward interpretation and mathematical properties, MSE serves as a critical evaluation criterion in the context of regression analysis and machine learning model performance assessment. MSE values vary depending on the context and application. Lower MSE values indicate that predictions are closer to the actual observations, making them generally more desirable (Nguyen et al., 2019).

The formula for MSE is expressed as follows:

$$\text{MSE} = \frac{1}{n} \sum_{i=1}^{n} (y_i - \hat{y}_i)^2 \quad (14)$$

- y_t: The actual (observed) value at time t,
- $\hat{y}_i$: The forecasted value at time t,
- n: The number of observations,

The root mean squared error (RMSE), similar to MSE, is a widely used error measurement method for evaluating how well predicted values align with actual observations. As a fundamental tool in fields such as machine learning, forecasting, and statistical analysis, RMSE is calculated by taking the square root of the mean of the squared errors. Since it is expressed in the same units as the modeled data, RMSE is straightforward to interpret and easy to understand. Although RMSE does not penalize large errors as strongly as MSE, it still reflects the model's sensitivity to prediction errors while maintaining interpretability due to its unit consistency with the data. This makes RMSE particularly useful for performance evaluations and model comparisons. In practice, RMSE is often used alongside other metrics, such as MSE, to provide a more comprehensive assessment of model performance (Abdelkader et al., 2023).

The formula for RMSE is expressed as follows:

$$\text{RMSE} = \sqrt{\sum_{i=1}^{n} \frac{(y_i - \hat{y}_i)^2}{n}} \quad (15)$$

- y_t: The actual (observed) value at time t,
- $\hat{y}_t$: The forecasted value at time t,
- n: The number of observations,

4. RESULTS AND DISCUSSION

In this section, the electricity production forecasting results obtained using four different methods (ARIMA, the PSO-Optimized Holt's Method, and two types of long short-term memory [LSTM] neural networks) were presented and comparatively evaluated. The analysis covered Turkey's total electricity generation as well as production from coal, natural gas, hydroelectric, and renewable energy sources. For each type of electricity production and for the total generation values, the forecasting models' performances were assessed using the MAPE, MSE, and RMSE metrics, and the strengths and weaknesses of the methods were comparatively discussed.

4.1. Results of ARIMA Models

As stated in pirivious section, the first step in determining the most appropriate ARIMA model for the series is to examine its

stationarity. For this purpose, an initial assessment is conducted using visual methods; the time series plot, together with the autocorrelation function (ACF) and partial autocorrelation function (PACF) plots, provides a preliminary indication of stationarity.

The time series plot of total energy generation data, presented in Figure 1, reveals a clear trend pattern. In addition, the ACF and PACF plots shown in Figure 2 further support the presence of a trend in the series. In particular, the ACF plot indicates that the autocorrelation values for the first few lags are relatively large and decline gradually, which clearly demonstrates that the series is non-stationary and exhibits trend behavior.

However, to obtain more reliable results, the visual inspection is supported by the Augmented Dickey-Fuller (ADF) unit root test. The null hypothesis (H_0) states that the series contains a unit root, i.e., it is non-stationary, while the alternative hypothesis (H_1) indicates that the series is stationary. The results of the test are summarized in Table 1.

Based on the results reported in Table 1, differencing was applied to the series in order to achieve stationarity. Stationarity was achieved after applying second-order differencing to the series. The corresponding ADF test results for the differenced series are reported in Table 2, and time series plot with ACF and PACF plots were given in Figure 3.

Figure 2: Time series plot of total energy generation

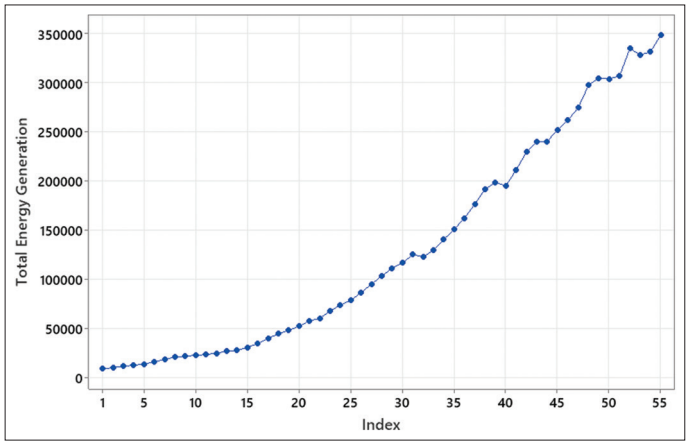

Table 1: ADF unit root test for the total electricity generation series

Test statistic	Critical value (5%)	P-value	Decision	Recommendation
−0.789	−2.930	0.822	Fail to reject H_0	Differencing is required to achieve stationarity

Table 2: ADF unit root test results for the differenced total electricity generation series

Test statistic	Critical value (5%)	P-value	Decision	Recommendation
−4,217	−2.930	0.001	Reject H_0	Data appears to be stationary, not supporting differencing

Considering the ACF and PACF plots in Figure 4 together with the theoretical autocorrelation patterns, the ARIMA (3,2,0) model was identified as the most suitable. The parameter estimates of this model are provided in Table 3.

As shown in Table 3, the estimated parameters of the proposed model are statistically significant, with all P-values being <0.05. As the next step, it is necessary to conduct diagnostic checks to assess whether the residuals from the fitted ARIMA model exhibit white noise behavior. For this purpose, the Ljung-Box Q-test is employed, and the corresponding results are reported in Table 4. The test statistic, with a $P \geq 0.05$, indicates that the model is appropriate for forecasting Total Electricity Generation.

For the other four series (coal, natural gas, hydroelectric, and renewable and waste-to-energy), the same Box-Jenkins procedure was applied. To avoid redundancy, only the final model specifications and diagnostic results are reported in Table 5.

The coal, natural gas, hydroelectric, and renewable and waste-to-energy electricity generation series all required second-order differencing to achieve stationarity. As summarized in Table 5, the most appropriate ARIMA specifications were identified as ARIMA(0,2,1) for coal, ARIMA(2,2,1) for natural gas, ARIMA(0,2,1) for hydroelectric, and ARIMA(0,2,3) for renewable and waste-to-energy. Diagnostic checks further confirmed the adequacy of these models (Table 5), with the residuals exhibiting no significant autocorrelation and thus approximating a white-noise process.

4.2. Results of LSTM Model

Two LSTM models were proposed for this study, both developed in the Python programming language. The models were trained and predictions were generated on a computer with a 64-bit operating system, equipped with an Intel Core i5-7200U processor at 2.50 GHz and 8 GB of RAM. Using the PyTorch deep learning library, these two LSTM models were developed to create separate forecasting models for total and four different electricity energy sources: Total, Coal, Natural Gas, Hydro, and Renewables and Waste. The models used annual electricity production data from 1970 to 2024 to generate future forecasts for 2025-2030, aiming for the lowest possible MAPE, MSE, and RMSE values. For input preparation, the data was partitioned by setting aside the last 3 years as a test set. MinMaxScaler was used to scale the data between 0 and 1.

Table 3: Parameter estimates of the ARIMA (3,2,0) model

Type	Coefficient	Standard error	t-value	P-value
AR (1)	−0.833	0.127	−6.54	0.000
AR (2)	−0.887	0.135	−6.59	0.000
AR (3)	−0.542	0.158	−3.42	0.001

Table 4: Results of the modified box-pierce (Ljung-Box) Chi-square test

Lag	Chi-square	Degrees of freedom (DF)	P-value
12	10.62	9	0.303
24	21.81	21	0.411
36	23.43	33	0.891
48	24.21	45	0.995

Figure 3: Autocorrelation function, and partial autocorrelation function plots for total energy generation

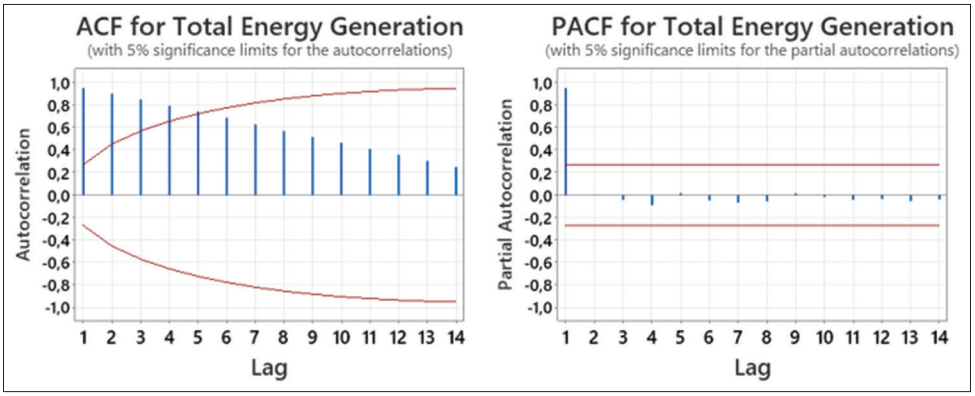

Figure 4: Time series, autocorrelation function and partial autocorrelation function plots for differenced total energy generation

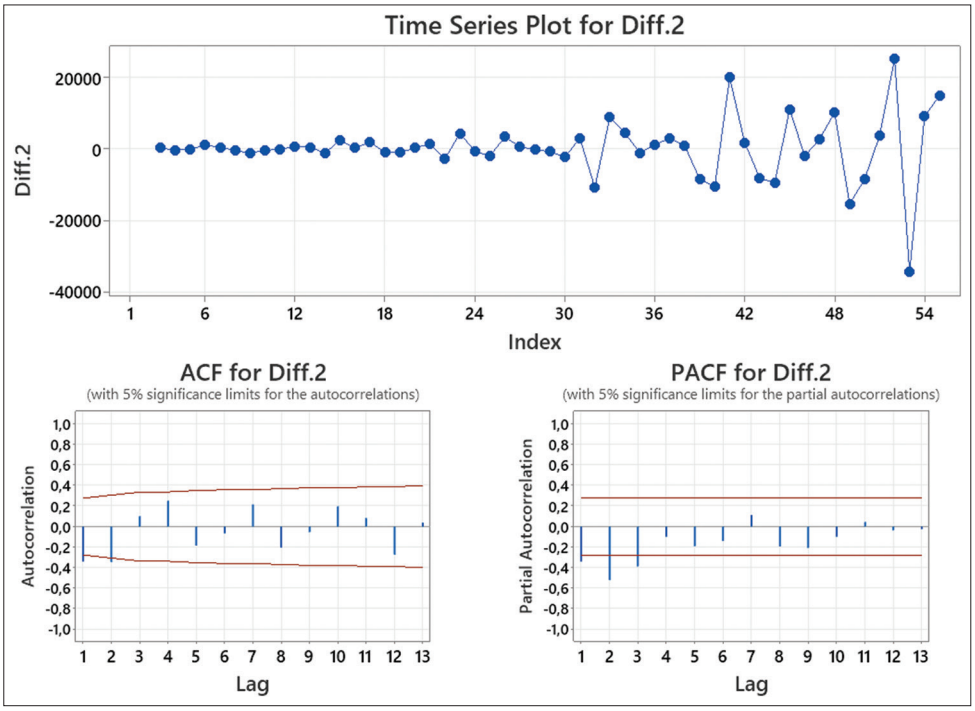

Table 5: ARIMA model specifications and diagnostic results for all electricity generation sources

Series	Model	Stationarity (ADF)	Ljung-Box P-values
Coal	ARIMA (0,2,1)	Stationary after 2nd diff. (P=0.000)	0.398; 0.689; 0.823; 0.985 (model adequate)
Natural gas	ARIMA (2,2,1)	Stationary after 2nd diff. (P=0.000)	0.723; 0.923; 0.993; 1.000 (model adequate)
Hydroelectric	ARIMA (0,2,1)	Stationary after 2nd diff. (P=0.000)	0.093; 0.513; 0.717; 0.970 (model adequate)
Renewable and waste	ARIMA (0,2,3)	Stationary after 2nd diff. (P=0.000)	0.947; 1.000; 1.000; 1.000 (model adequate)

The single-layer LSTM model architecture consists of a single LSTM layer with 50 hidden units, followed by a linear output layer. This model takes the input data, passes it directly through the LSTM layer to learn sequential dependencies, and then sends its output to a linear layer to generate a prediction.

The three-layer LSTM model architecture passes the input data sequentially through three different LSTM layers, each containing 50 hidden units. Each layer takes the output of the previous layer as its input. The first layer learns fundamental patterns in the time series, such as trend and seasonality. The second layer uses the output of the first layer to learn more complex, abstract, and hidden patterns. The third layer learns the most complex and long-term dependencies to prepare the final output.

Both models were trained with the same data preparation and training parameters: MinMaxScaler, MSE loss, Adam optimization, and different epoch number (500, 1000, 1500, 2000, 2500, 3000, 3500, and 4000). Model performance was evaluated by comparing the predictions on the test set with the actual values, using MAPE, RMSE, and MSE as evaluation metrics.

Future predictions (2025-2030) were made using a recursive process where the last known data point (2024) was used as the

input, and the model's output for one step became the input for the next. All results were supported by visualization tools, with graphs presenting historical data, test predictions, and future forecasts.

Table 6 presents the results obtained from LSTM models with varying numbers of layers and epochs. Due to their inherent nature, LSTM models produce somewhat random results in each run. However, the success of the resulting solutions is significantly influenced by the dataset's structure and the number of epochs. For the total energy production dataset, both LSTM models performed exceptionally well. The 3-layer LSTM, in particular, delivered a superior solution with a near-zero error rate at a higher epoch count. Regarding the coal dataset, which exhibits minor fluctuations over the years, the 1-layer LSTM model generally struggled to capture these details. In contrast, increasing the number of layers enabled the model to effectively capture these fluctuations, even at low epoch values. The 3-layer LSTM provided an excellent forecast with a very low, almost zero, error rate. The natural gas data presented a challenge for the LSTM model due to the limited number of data points. Nevertheless, an acceptable forecasting model was achieved with a MAPE error rate of 14%.

For the hydroelectric data, where minimal year-over-year variation was observed, the error rate increased as both the number of epochs and layers were raised. This outcome indicates that the models were overfitting, or memorizing the data rather than learning its underlying patterns. Consequently, for this specific dataset, a low number of layers and approximately 1,000 epochs were found to be most suitable. The data for renewable energy and waste initially showed a declining trend over the years, followed by a period of rapid growth. The 1-layer LSTM model was able to capture this volatile structure with a very low error rate at a high epoch count of 4,000. It's important to note that the mean absolute percentage error (MAPE) could not be calculated for this dataset due to the presence of zero values. Furthermore, an examination of Table 6 reveals that the solution time for LSTM models significantly increases with both the number of layers and the number of epochs. While a higher epoch count can be advantageous for capturing intricate details in datasets, it can also lead to overfitting when applied to datasets with fewer details or less complexity. This causes the algorithm to memorize the training data rather than generalize effectively to new data.

An analysis of Figure 5 indicates that the number of layers, the number of epochs, and the characteristics of the dataset all significantly influence the training time and performance of the model. The figure clearly demonstrates that for each dataset, increasing the number of LSTM layers leads to longer training and solution times. Furthermore, a linear increase between the number of epochs and the solution time is clearly observed for both the 1- and 3-layer LSTM models. The performance of the LSTM models varies depending on the structure of the dataset. It was observed that increasing the number of epochs and layers did not consistently improve the model's performance. Therefore, accurately determining the optimal number of epochs and layers is crucial for achieving the best results. When examining the time-series data for total energy production, the 1-layer LSTM model yielded near-perfect results at 1,500 epochs, while the 3-layer LSTM model performed best at 2,500 epochs. However, it is understood that the slightly superior performance of the 3-layer LSTM model at this epoch count suggests a potential for overfitting beyond this point.

In the case of electricity production data from coal, the performance of the 1-layer LSTM model progressively worsened as the number of epochs increased. In contrast, the 3-layer model occasionally found good results due to randomness and showed its best performance at 1,500 epochs, producing highly successful results with a near-zero MAPE value. However, the 1-layer model exhibited a strong overfitting tendency at 2,000 and higher epochs. While significant improvement was recorded at 1,000 and 1,500 epochs, a sharp deterioration in RMSE and MAPE values occurred after 2,000 epochs.

For models developed to predict electricity production from natural gas, the best performance was achieved with the 3-layer model at 3,000 epochs (RMSE: 9293.28, MAPE: 14.09%). However, both models showed a tendency towards overfitting after 3,000 epochs. It is thus clear that using a higher number of epochs beyond 3,000 does not provide any advantage in terms of prediction performance.

When analyzing hydroelectric data, the 1-layer LSTM model was found to be more successful at capturing the dataset's characteristics. It performed best at 1,000 epochs, with an RMSE of 1086.99 and a MAPE of 1.45%. However, it was observed that as the number of epochs increased, the 1-layer model shifted from learning to memorizing the data, leading to overfitting after 1,500 epochs. Although the 3-layer model showed some improvement as the number of epochs increased, the 1-layer model's success in capturing the dataset's trend was more notable.

Table 6: LSTM models, epoch numbers, exectution time and the best RMSE and best MAPE

Energy source	Model architecture	Best epoch number	Training time (s)	Best RMSE	Best MAPE (%)
Total	1-Layer LSTM	1500	152.45	3,427.55	0.98
	3-Layer LSTM	2500	492.19	215.56	0.06
Coal	1-Layer LSTM	500	46.79	28,720.66	23.39
	3-Layer LSTM	1500	288.70	168.06	0.14
Natural gas	1-Layer LSTM	3500	320.47	17,904.90	27.15
	3-Layer LSTM	3000	559.81	9,293.28	14.09
Hydro	1-Layer LSTM	1000	91.40	1,086.99	1.45
	3-Layer LSTM	3500	655.73	8,886.68	11.85
Renewable energy	1-Layer LSTM	4000	366.41	1,900.35	-
	3-Layer LSTM	1000	185.08	22,775.49	-

Figure 5: Analysis of long short-term memory model performance with epoch number, time and root mean squared error

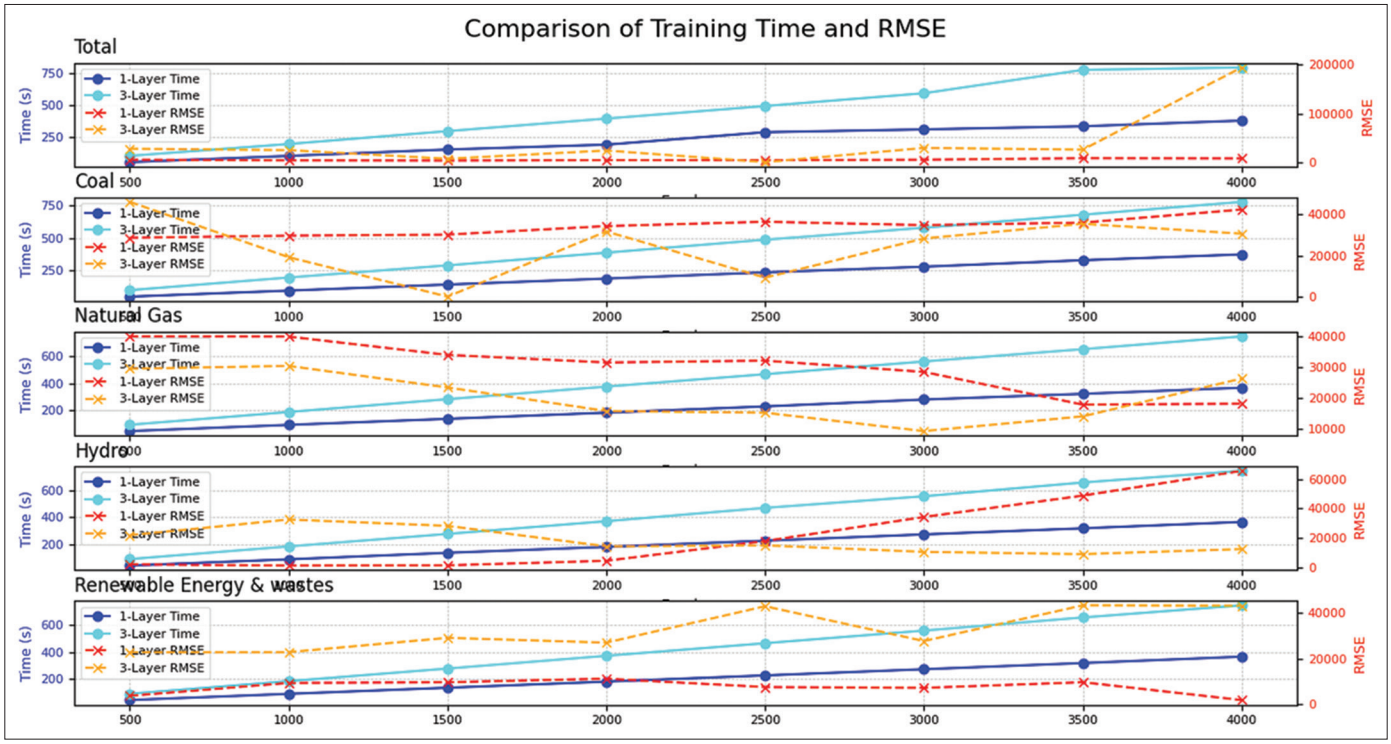

A different situation was observed with the electricity production data from renewable energy and waste. The 1-layer model achieved its best result at 4,000 epochs (RMSE: 1900.35, MAPE: 2.23%). This is a rare occurrence, as the increased number of epochs unexpectedly led to better performance in this specific case.

Due to the relatively small size of the datasets, the LSTM model shows significant overfitting at large epoch values. The performance of the 3-layer LSTM was initially low, remained unstable during training, and resulted in high error rates. This highlights that a higher number of layers is not always suitable and that determining the appropriate number of layers and epochs based on the specific dataset is crucial. For the total energy, coal, and natural gas datasets, the optimal training point was found at relatively low epoch values, after which the model's performance declined. During the LSTM training process, validation metrics were carefully monitored, and an appropriate stopping point was determined to prevent overfitting.

Table 7 presents the results obtained from LSTM models with varying numbers of layers and epochs. Due to their inherent nature, LSTM models produce somewhat random results in each run. However, the success of the resulting solutions is significantly influenced by the dataset's structure and the number of epochs. For the total energy production dataset, both LSTM models performed exceptionally well. The 3-layer LSTM, in particular, delivered a superior solution with a near-zero error rate at a higher epoch count. Regarding the coal dataset, which exhibits minor fluctuations over the years, the 1-layer LSTM model generally struggled to capture these details. In contrast, increasing the number of layers enabled the model to effectively capture these fluctuations, even at low epoch values. The 3-layer LSTM provided an excellent forecast with a very low, almost zero, error rate. The natural gas data presented a challenge for the LSTM model due to the limited number of data points. Nevertheless, an acceptable forecasting model was achieved with a MAPE error rate of 14%.

For the hydroelectric data, where minimal year-over-year variation was observed, the error rate increased as both the number of epochs and layers were raised. This outcome indicates that the models were overfitting, or memorizing the data rather than learning its underlying patterns. Consequently, for this specific dataset, a low number of layers and approximately 1,000 epochs were found to be most suitable.

The data for renewable energy and waste initially showed a declining trend over the years, followed by a period of rapid growth. The 1-layer LSTM model was able to capture this volatile structure with a very low error rate at a high epoch count of 4,000. It's important to note that the mean absolute percentage error (MAPE) could not be calculated for this dataset due to the presence of zero values. Furthermore, an examination of Table 7 reveals that the solution time for LSTM models significantly increases with both the number of layers and the number of epochs. While a higher epoch count can be advantageous for capturing intricate details in datasets, it can also lead to overfitting when applied to datasets with fewer details or less complexity. This causes the algorithm to memorize the training data rather than generalize effectively to new data.

4.3. Results of PSO-Optimized Holt's Model

In this study, the Holt forecasting method was used to predict the future values of the data. However, the most critical point for this method is determining the correct α and β coefficients. To find the lowest possible MAPE, MSE, and RMSE values, the PSO algorithm, which has been shown to yield successful results in the literature, was used.

Table 7: LSTM models, epoch numbers, exectution time and the best RMSE and best MAPE

Energy source	Model architecture	Best epoch number	Training time (s)	Best RMSE	Best MAPE (%)
Total	1-Layer LSTM	1500	152.45	3,427.55	0.98
	3-Layer LSTM	2500	492.19	215.56	0.06
Coal	1-Layer LSTM	500	46.79	28,720.66	23.39
	3-Layer LSTM	1500	288.70	168.06	0.14
Natural gas	1-Layer LSTM	3500	320.47	17,904.90	27.15
	3-Layer LSTM	3000	559.81	9,293.28	14.09
Hydro	1-Layer LSTM	1000	91.40	1,086.99	1.45
	3-Layer LSTM	3500	655.73	8,886.68	11.85
Renewable energy	1-Layer LSTM	4000	366.41	1,900.35	-
	3-Layer LSTM	1000	185.08	22,775.49	-

The model was developed in Python. Model training and forecasting were carried out on a 64-bit operating system with an Intel Core i5-7200U processor running at 2.50 GHz and 8 GB of RAM. Using annual electricity production data from 1970 to 2024, forecasting models were developed for five different energy sources for the future: Total, Coal, Natural Gas, Hydro, and Renewable Energy and Waste. The goal of the model is to produce future forecasts for the years 2025-2030 with the lowest MAPE, MSE, and RMSE values.

w,c1 and c2 parameters are crucial and the parameter values are w=0.7, c1=2.0, c2=2.0 which are standard choices in PSO literature and generally provide good performance across a wide range of optimization problems, which is why they were selected for this implementation in this study. The steps of particle swarm optimization (PSO) was used to optimize the parameters of the Holt forecasting model are shown below:

- Step 1. Initialization
- Step 2. Load dataset (Total, Coal, Hydro, Natural Gas, Renewable&Waste.).
- Step 3. Initialize PSO (particles:100, 200, 300, 400, 500), iterations:10, 100, 1000 α, β).
- Step 4. Evaluate fitness (MSE) for each particle.
- Step 5. Update pbest and gbest.
- Step 6. Iterate until stopping criterion.
- Step 7. Return optimal α, β.
- Step 8. Apply Holt forecasting with optimal parameters.
- Step 9. Compute error metrics (MSE, RMSE, MAPE).
- Step 10. Forecast future values (until 2030).
- Step 11. Save and visualize results.

Table 8 presents the optimal (α) and (β) coefficient values for various datasets, as determined by the Particle Swarm Optimization (PSO) algorithm used to optimize the Holt's Linear trend model. The analysis section details the optimal α and β values found for specific initial population and iteration counts. The study investigated the effect of the initial population size (100, 200, 300, 400, and 500) and the number of iterations (10, 100, and 1,000) on the quality of the solution. The quality was assessed by evaluating the RMSE values. The results presented below were obtained from three separate runs of the PSO-optimized Holt's Linear Trend model. Despite its stochastic nature, the model demonstrated a robust solution structure, consistently finding values that were nearly identical, with only negligibly small differences.

Upon examining the table, it was observed that the algorithm generally reached the optimal α and β values with 100 particles and 100 iterations. Even an initial particle count of 10 was sufficient. Increasing the particle count up to 500 and the iteration count to 1,000 is unnecessary for the PSO algorithm in this specific problem and dataset. In fact, for the electricity generation data from renewable energy and waste, it was found that an initial population as low as 10 particles and 100 iterations was sufficient to reach the optimum solution. Running the algorithm beyond these values did not result in any change in its performance. Furthermore, the consistency of results across a wide range of population sizes (100-500) indicates that the PSO is robust for this application and the solution space likely has a well-defined global minimum of RMSE.

In Holt's Linear Trend model, the α and β coefficients are smoothing parameters that control how the developed model responds to changes in the base level and trends in the time series data to provide the forecast with the lowest error. The α coefficient, also known as the Level Component, indicates that values closer to 1 mean more weight is given to the most recent observations in the model, resulting in greater sensitivity to rapid changes in the level. Conversely, values closer to 0 indicate that the model gives more weight to the historical average and responds more slowly to changes in the level. The B (β) Coefficient determines how quickly the model responds to changes in the trend. Values closer to 1 indicate a rapid response to trend changes, while values closer to 0 indicate a slower response to trend changes and a more stable trend.

According to Table 8, the α value of 0.6 for the model predicting total electrical energy level shows that the model values both recent and past data. The model's β value of 0.21 indicates that the trend component is quite stable and insensitive to sudden changes in the trend. For the electricity generation dataset from coal, a very high α value (0.9619) was found. This value indicates that the model is very sensitive to the most recent observations and that the level can change rapidly. However, the very low β value (0.0768) shows that the trend changes very slowly and is almost constant. For the natural gas energy dataset, the α value is low at 0.1776. This indicates that the model relies more on the historical average. In contrast, the β value of 1.0000 means it responds instantly to changes in the trend. For the renewable energy and waste dataset, the α value is at the maximum of 1.0000, showing the model is based entirely on the most recent observations. The β value of 0.5856 indicates a rapid response to trend changes. These parameter values show that the PSO algorithm optimized

Table 8: Convergence behavior and optimal parameters of the PSO algorithm for the holt linear trend model

Energy source	Optimal α	Optimal β	Best RMSE	Best MAPE (%)	RMSE ımprovement (10 vs. 100 Iter.)	Converges at (Iterations)	Min. effective Pop. size
Total	0.6010	0.2099	5,947.87	3,58	Negligible	100	100
Coal	0.9619	0.0768	4,694.86	9,01	Negligible	100	100
NaturaGas	0.1776	1.0000	12,036.9	24,20	Negligible	100	100
Hydro	0.3595	0.0708	7,888.31	19,95	Negligible	100	100
Renewable and wastes	1.0000	0.5856	1,281.28	-	None	10	100

them according to the unique time series characteristics of each energy source dataset.

5. COMPARISON OF FORECASTING MODELS

This section evaluates the forecasting performance of the developed models. Model comparisons were conducted based on MSE, RMSE and MAPE errors across five distinct electricity energy production datasets. In order to enhance the reliability of the results for LSTM and PSO Optimised Holt models, each was run multiple times, and the average MAPE, RMSE, and MSE values were reported.

Table 9 provided a comprehensive comparison of the forecasting performance of different time-series models ARIMA, 1-Layer LSTM, 3-Layer LSTM, and PSO-Optimized Holt method for Turkey's total electricity generation as well as for Coal, Natural Gas, Hydroelectric, and Renewable and Waste energy sources. The performance metrics used, MSE, RMSE, and MAPE, objectively indicated the accuracy levels of the models. In the table, values highlighted in bold represented the best-performing method for each energy source. For the Renewable and Waste category, MAPE values could not be calculated due to the presence of zero values in the dataset.

The results indicated that the 3-Layer LSTM model demonstrated a clear superiority over the other methods for total electricity generation (MSE = 46,463.31; MAPE = 0.06). Similarly, for coal-based generation, the 3-Layer LSTM model stood out with a very low error rate. For natural gas, although the 3-Layer LSTM model provided the lowest MSE, the MAPE was found to be 14.09%, suggesting that this energy source was relatively more difficult to predict. In the case of hydroelectric generation, the 1-Layer LSTM model achieved the lowest MSE and MAPE (1.45%), distinguishing itself from the other methods. In contrast, the ARIMA model exhibited the best performance for renewable and waste-based energy sources.

Overall, it was observed that deep learning-based LSTM methods demonstrated strong performance in capturing the complex dynamics of electricity generation. At the same time, it is noteworthy that traditional methods such as ARIMA were still able to achieve high accuracy for certain energy types (e.g., renewable and waste). The fact that the MAPE values for all methods remained below 5% confirmed that the models generally provided acceptable and highly accurate forecasts. These findings indicate that the choice of forecasting method in electricity generation studies may vary depending on the data structure and the characteristics of the energy source.

Table 9: Forecasting errors for total electricity generation and its sources using ARIMA, PSO-optimized holt, 1-Layer, and 3-Layer LSTM methods

Electrıcity source	Model	MSE	RMSE	MAPE (%)
Total	ARIMA (3,2,0)	34,982,567.00	5,914.60	3.12
	1-Layer LSTM	11,747,088.00	3,427.55	0.98
	3-Layer LSTM	46,463.31	215.56	0.06
	PSO Opt. Holt	35,376,089.00	5,947.87	3.67
Coal	ARIMA (1,2,0)	22,758,635.00	4,770.60	11.30
	1-Layer LSTM	824,957,318.00	28,720.66	23.39
	3-Layer LSTM	28,257.63	168.06	0.14
	PSO Opt. Holt	22,044,703.00	4,694.86	8.92
Natural gas	ARIMA (2,2,1)	131,340,310.00	11,460.38	16.10
	1-Layer LSTM	320,616,181.00	17,904.90	27.15
	3-Layer LSTM	86,360,739.00	9,293.28	14.09
	PSO Opt. Holt	144,886,656.00	12,036.90	24.19
Hydro	ARIMA (0,2,1)	78,464,995.00	8,850.00	17.38
	1-Layer LSTM	1,181,560.00	1,086.99	1.45
	3-Layer LSTM	78,969,329.00	8,886.68	11.85
	PSO Opt. Holt	62,238,981.00	7,888.31	18.47
Renewable and wastes	ARIMA (0,2,2)	1,308,641.00	1,143.96	–
	1-Layer LSTM	3,611,330.00	1,900.35	–
	3-Layer LSTM	518,456,657.00	22,775.49	–
	PSO Opt. Holt	1,641,679.00	1,281.28	–

Based on the examination of Table 10, the forecast values for the period between 2025 and 2030 were obtained using the method that produced the lowest error value. The findings provide valuable insights into the prospective dynamics of the national energy portfolio. The results indicate that total electricity generation is expected to follow a steady and significant upward trajectory throughout this period. Specifically, according to the forecasts obtained from the 3-Layer LSTM model, total production is projected to reach 369,155 GWh in 2025 and to increase to 439,104 GWh by 2030. This upward trend can be interpreted as an indicator of expanding energy investments.

When analyzing the distribution of sub-energy sources, coal and hydroelectric power are projected to maintain a relatively stable trajectory over the forecast horizon. Specifically, coal-based electricity generation is expected to decline modestly, from 122,214 GWh in 2025 to 118,938 GWh in 2030, suggesting that reliance on coal will not intensify and will likely remain at current levels. Hydroelectric production, while subject to minor fluctuations driven by climatic conditions (e.g., the temporary decline anticipated in 2026), is forecasted to remain broadly stable at around 70,000 GWh.

Tablo 10: Forecasts for the energy datasets for 2025-2030 in gwh using the method with the lowest error value

Resource (Method)\Year	2024*	2025	2026	2027	2028	2029	2030
Total (3-Layer LSTM)	348 900	369 155	386 801	396 781	406 681	421 568	439 104
Coal (3-Layer LSTM)	122813	122 214	120 762	119 280	118 659	118 636	118 938
Natural gas (3-Layer LSTM)	65942	101 029	98 412	98 360	96 273	99 019	109 878
Hyro (1-Layer LSTM)	75014	76018	68039	70368	69197	72166	74133
Renewable ENG and waste (ARIMA [0, 2, 2])	85132	92 431	99 730	107 029	114 328	121 628	128 927

In contrast, the forecast values for natural gas and renewable energy highlight their role as the primary drivers of the projected increase in total electricity generation. Natural gas output is anticipated to grow from 101,029 GWh in 2025 to 109,878 GWh in 2030, reflecting considerable growth potential. This trend underscores the likelihood that natural gas will function as a transitional energy source in the coming years, offering a comparatively cleaner fossil fuel alternative to coal. The projections for renewable energy and energy derived from waste (Table 9) reveal the most striking development: an exceptionally robust and sustained growth pattern. Total generation from these sources is expected to expand from 92,431 GWh in 2025 to 128,927 GWh in 2030, marking the fastest and most consistent increase among all electricity sources. These findings clearly indicate a structural shift in energy policies and investments toward renewable resources, pointing to a rapid expansion of capacity in this sector.

6. CONCLUSION

In this study, a multi-methodological approach was presented for forecasting Turkey's electricity generation. By analyzing electricity production data from 1970 to 2024, forecasts were made for total electricity generation as well as for individual energy sources Coal, Natural Gas, Hydroelectric, Renewable, and Waste-based energy. The main objective of the study is to compare the forecasting performance of traditional statistical methods such as the Box-Jenkins ARIMA model, optimization-based approaches like the PSO-optimized Holt Linear Trend method, and modern deep learning algorithms (1-layer and 3-layer LSTM models), and to comprehensively reveal Turkey's projected electricity generation progress up to 2030. This research holds significant importance for energy policy-making, investment planning, and the establishment of sustainability goals.

The overall findings of the study indicate that model performance is highly dependent on the dataset, demonstrating that the best-performing model varies according to the structure of the data. The results show that each methodology exhibits different performance levels depending on the unique characteristics (trend, data volume) of the dataset corresponding to each electricity source.

For Total Electricity Generation, Coal, and Natural Gas production forecasts, the 3-Layer LSTM model achieved the lowest error metrics (MSE, RMSE, and MAPE) due to its ability to capture complex and nonlinear dynamics in the data, thereby demonstrating the best performance. In the case of Hydroelectric power generation, which has a relatively simpler structure, the 1-Layer LSTM model provided the most successful results. This finding suggests that simpler architectures can be sufficient for less volatile series, and that model complexity should not be unnecessarily increased. For Renewable Energy and Waste-based electricity generation, the ARIMA method proved to be the most effective, as it best modeled the initially decreasing but later exponentially increasing trend observed in recent years. This result confirms that traditional time-series methods can still be effectively utilized for datasets exhibiting strong and consistent trends. Although the PSO-optimized Holt Linear Trend method did not achieve the best performance in any specific category, it consistently produced reliable and acceptable forecasts across all categories, proving to be a stable and dependable alternative method.

The policy and practical implications of this study were highly significant. Based on model-based forecasts, a steady increase in Turkey's total electricity generation is projected for the 2025–2030 period. However, to prevent this growth from lagging behind the rate of consumption increase projected in the National Energy Plan, it is essential to accelerate investments in energy production capacity. The sharp upward trend forecasted for renewable energy generation support the view that the efforts in this area were promising. Furthermore, the continued increase in natural gas-based generation suggests that natural gas will maintain its role as a "transition fuel", serving as a cleaner fossil fuel alternative to coal.

The main limitation of this study was that the forecasts rely solely on historical annual data trends. Future uncertainties such as policy changes, the commissioning of nuclear power plants, technological advancements, global economic crises, or climate events may affect the accuracy of these forecasts. Such external factors could potentially constrain the future performance of the model.

In conclusion, this study strongly emphasizes that there is no single universal model for energy forecasting. To achieve optimal forecasting performance, it is crucial to select the model in accordance with the historical data structure and dynamics of each energy source and to perform hyperparameter optimization, especially in deep learning models. This research provides a solid foundation for decision-makers and energy planners to employ a hybrid modeling framework capable of generating reliable forecasts under different scenarios. Ultimately, this study not only provides concrete projections for the future trajectory of Turkey's electricity generation, but also makes a valuable contribution to the methodological discourse in the field of forecasting modeling. The findings reaffirm the critical importance of accurate planning in achieving Turkey's energy independence and sustainability goals.

The main limitation of this study was that the forecasts rely solely on historical annual data trends. Future uncertainties such as policy changes, the commissioning of nuclear power plants, technological advancements, global economic crises, or climate events may

affect the accuracy of these forecasts. Such external factors could potentially constrain the future performance of the model.

Future research could focus on developing a more comprehensive forecasting framework by integrating these models with economic, demographic, and climatic variables. To improve the accuracy of forecasts, external factors such as renewable energy investment levels, GDP, population growth, weather data, reservoir water levels, natural gas prices, and coal import/export volumes can be incorporated into the models. Parameter optimization of Holt or other time-series models could be explored using different metaheuristic algorithms (e.g., Genetic Algorithms, Differential Evolution). Utilizing high-frequency data (daily or weekly) would allow for a more precise capture of seasonal and cyclical patterns. Moreover, constructing hybrid forecasting models that combine the strengths of different methods could further enhance prediction accuracy. Investigating the performance of more advanced artificial intelligence-based architectures would also make a valuable contribution to this field.

REFERENCES

Abdelkader, E.M., Elshaboury, N., Ali, E., Alfalah, G., Mansour, A., Alsakkaf, A. (2023), A Hyper Parametrized Deep Learning Model for Analyzing Heating and Cooling Loads in Energy Efficient Buildings. In: Proceedings of the International Conference on New Trends in Applied Sciences.

Acar, B., Yiğit, S., Tuzuner, B., Özgirgin, B., Ekiz, İ., Özbiltekin-Pala, M., Ekinci, E. (2021), Electricity consumption forecasting in Turkey. In: Digitizing Production Systems: Selected Papers from ISPR2021, Turkey, Springer. p702-714.

Akarsu, G. (2017), Forecasting regional electricity demand for Turkey. International Journal of Energy Economics and Policy, 7(4), 275-282.

Akay, D., Atak, M. (2007), Grey prediction with rolling mechanism for electricity demand forecasting of Turkey. Energy, 32(9), 1670-1675.

Akdağ, H., Ekici, H. (2022), Türkiye'de enerji üretim ve tüketiminin sanayi endeksi üzerindeki etkisi. Adnan Menderes Üniversitesi Sosyal Bilimler Enstitüsü Dergisi, 9(2), 103-112.

Al-hamid, A.H.M., Savaş, S. (2023), A deep learning approach to real-time electricity load forecasting. Journal of Information Systems and Management Research, 5(2), 1-9.

Atilgan, B., Azapagic, A. (2016), An integrated life cycle sustainability assessment of electricity generation in Turkey. Energy Policy, 93, 168-186.

Bakay, M.S., Ağbulut, Ü. (2021), Electricity production based forecasting of greenhouse gas emissions in Turkey with deep learning, support vector machine and artificial neural network algorithms. Journal of Cleaner Production, 285, 125324.

Bişkin, O.T., Çifçi, A. (2021), Forecasting of Turkey's electrical energy consumption using LSTM and GRU networks. Bilecik Şeyh Edebali Üniversitesi Fen Bilimleri Dergisi, 8(2), 656-667.

Buhan, I., Batina, L., Yarom, Y., Schaumont, P. (2022), SoK: Design Tools for Side-Channel-Aware Implementations. In: Proceedings of the 2022 ACM on Asia Conference on Computer and Communications Security.

Bulut, M. (2024), Improving deep learning forecasting model based on LSTM for Türkiye's hydro-electricity generation. Sakarya University Journal of Computer and Information Sciences, 7(3), 325-337.

Chairunnisa, A.D.A., Fauzan, A. (2023), Implementation of panel data regression in the analysis of factors affecting poverty levels in Bengkulu province in 2017-2020: Implementation of panel data regression. EKSAKTA: Journal of Sciences and Data Analysis, 4, 40-45.

Dobre, I., Alexandru, A. (2008), Modelling unemployment rate using Box-Jenkins procedure. Journal of applied quantitative methods, 3(2), 156-166.

Dritsakis, N., Klazoglou, P. (2018), Forecasting unemployment rates in USA using Box-Jenkins methodology. International Journal of Economics and Financial Issues, 8(1), 9.

Ebesek, Ö.T., Ebesek, Ş. (2023), Optimizing holt-winters exponential smoothing parameters for construction cost index forecasting with PSO and walk-forward cross-validation. Kent Akademisi, 16(4), 2422-2439.

Ertekin, S. (2020), Solar power prediction with an hour-based ensemble machine learning method. Hittite Journal of Science and Engineering, 7(1), 35-40.

Günay, M.E. (2016), Forecasting annual gross electricity demand by artificial neural networks using predicted values of socio-economic indicators and climatic conditions: Case of Turkey. Energy Policy, 90, 92-101.

Hakimah, M., Kurniawan, M. (2020), Integration of double exponential smoothing damped trend with metaheuristic methods to optimize forecasting rupiah exchange rate against USD during COVID-19 pandemic. Khazanah Informatika: Jurnal Ilmu Komputer dan Informatika, 6(2), 151-7.

Haliloğlu, E.Y., Tutu, B.E. (2018), Forecasting daily electricity demand for Turkey. Turkish Journal of Energy Policy, 3(7), 40-49.

Hamzaçebi, C. (2007), Forecasting of Turkey's net electricity energy consumption on sectoral bases. Energy Policy, 35(3), 2009-2016.

Hamzaçebi, C., Es, H.A., Çakmak, R. (2019), Forecasting of Turkey's monthly electricity demand by seasonal artificial neural network. Neural Computing and Applications, 31(7), 2217-2231.

Hanke, J. E., Wichern, D. (2014), Business Forecasting. Pearson Education.

Holt, C.C. (2004), Forecasting seasonals and trends by exponentially weighted moving averages. International Journal of Forecasting, 20(1), 5-10.

Inglesi-Lotz, R. (2016), The impact of renewable energy consumption to economic growth: A panel data application. Energy Economics, 53, 58-63.

Institute, T.S. (2025). Available from: https://www.tuik.gov.tr [Last accessed on 2025 Jul 22].

Jiang, H., He, Z., Ye, G., Zhang, H. (2020), Network intrusion detection based on PSO-XGBoost model. IEEE Access, 8, 58392-58401.

Kankal, M., Uzlu, E. (2017), Neural network approach with teaching–learning-based optimization for modeling and forecasting long-term electric energy demand in Turkey. Neural Computing and Applications, 28(Suppl 1), 737-747.

Kaytez, F. (2020), A hybrid approach based on autoregressive integrated moving average and least-square support vector machine for long-term forecasting of net electricity consumption. Energy, 197, 117200.

Kennedy, J., Eberhart, R. (1995), Particle Swarm Optimization. In: Proceedings of ICNN'95-International Conference on Neural Networks.

Kıran, M.S., Özceylan, E., Gündüz, M., Paksoy, T. (2012), Swarm intelligence approaches to estimate electricity energy demand in Turkey. Knowledge-Based Systems, 36, 93-103.

Kurt, E., Kasap, R., Çelik, K. (2022), Forecasting of monthly electricity generation from the conventional and renewable resources following the corona virus pandemic in Turkey. Journal of Energy Systems, 6(3), 420-435.

Lucia, U., Grisolia, G. (2017), Biothermoeconomics Analysis of Cyanobacteria and Microalga Use for Sustainable Biofuel. arXiv preprint arXiv:1710.00660.

Matrenin, P., Sekaev, V. (2015), Particle Swarm Optimization with Velocity Restriction and Evolutionary Parameters Selection for Scheduling Problem. In: 2015 International Siberian Conference on Control and Communications (SIBCON).

Meyr, H. (2014), Forecast methods. In: Supply Chain Management and Advanced Planning: Concepts, Models, Software, and Case Studies. Berlin: Springer. p513-523.

Nguyen, V.V., Pham, B.T., Vu, B.T., Prakash, I., Jha, S., Shahabi, H., Shirzadi, A., Ba, D.N., Kumar, R., Chatterjee, J.M. (2019), Hybrid machine learning approaches for landslide susceptibility modeling. Forests, 10(2), 157.

Notton, G., Nivet, M.L., Voyant, C., Paoli, C., Darras, C., Motte, F., Fouilloy, A. (2018), Intermittent and stochastic character of renewable energy sources: Consequences, cost of intermittence and benefit of forecasting. Renewable and Sustainable Energy Reviews, 87, 96-105.

Oscar, N. (2021). Multivariate Short-term Electricity Load Forecasting with Deep Learning and exogenous covariates. Umeå University, Faculty of Science and Technology, Department of Applied Physics and Electronics, Master's Thesis (MSc in Energy Engineering), 37.

Owusu, P.A., Asumadu-Sarkodie, S. (2016), A review of renewable energy sources, sustainability issues and climate change mitigation. Cogent Engineering, 3(1), 1167990.

Özbay, H., Dalcali, A. (2021), Effects of COVID-19 on electric energy consumption in Turkey and ANN-basedshort-term forecasting. Turkish Journal of Electrical Engineering and Computer Sciences, 29(1), 78-97.

Pangestu, A.I., Andayani, P. (2023), Implementation of holt-winter exponential smoothing method to forecast the spread of Covid-19. Indonesian Journal of Mathematics and Applications, 1(2), 13-24.

Paul, D.I., Uhomoibhi, J. (2012), Solar power generation for ICT and sustainable development in emerging economies. Campus-Wide Information Systems, 29(4), 213-225.

Ran, X., Shan, Z., Fang, Y., Lin, C. (2019), An LSTM-based method with attention mechanism for travel time prediction. Sensors, 19(4), 861.

Ren, Z., Zhang, S., Liu, H., Huang, R., Wang, H., Pu, L. (2024), The feasibility and policy engagements in achieving net zero emission in China's power sector by 2050: A LEAP-REP model analysis. Energy Conversion and Management, 304, 118230.

Resources. (2025). Available from: https://enerji.gov.tr [Last accessed on 2025 Jul 22].

Saglam, M., Spataru, C., Karaman, O.A. (2023), Forecasting electricity demand in Turkey using optimization and machine learning algorithms. Energies, 16(11), 4499.

Şahin, U. (2020), Projections of Turkey's electricity generation and installed capacity from total renewable and hydro energy using fractional nonlinear grey Bernoulli model and its reduced forms. Sustainable Production and Consumption, 23, 52-62.

Soğukpınar, F., Erkal, G., Özer, H. (2023), Evaluation of renewable energy policies in Turkey with sectoral electricity demand forecasting. Environmental Science and Pollution Research, 30(13), 35891-35912.

Tak, N., Egrioglu, E., Bas, E., Yolcu, U. (2021), An adaptive forecast combination approach based on meta intuitionistic fuzzy functions. Journal of Intelligent and Fuzzy Systems, 40(5), 9567-9581.

Ugurlu, U., Tas, O., Gunduz, U. (2018), Performance of electricity price forecasting models: Evidence from turkey. Emerging Markets Finance and Trade, 54(8), 1720-1739.

Voloshko, A., Bederak, Y., Kozlovskyi, O. (2019), An improved pre-forecasting analysis of electrical loads of pumping station. Resource-Efficient Technologies, 4, 20-29.

Wu, M., Du, P., Jiang, M., Goh, H.H., Zhu, H., Zhang, D., Wu, T. (2022), An integrated energy system optimization strategy based on particle swarm optimization algorithm. Energy Reports, 8, 679-691.

Yapar, G., Capar, S., Selamlar, H.T., Yavuz, I. (2018), Modified holt's linear trend method. Hacettepe Journal of Mathematics and Statistics, 47(5), 1394-1403.

Yildizhan, H., Sivrioğlu, M. (2015), Electricity generation by solar energy in Turkey: Current state and outlook. Journal of Energy and Power Engineering, 9, 1093-1100.

Yılmaz, B. (2023), Generative adversarial network for load data generation: Türkiye energy market case. Mathematical Modelling and Numerical Simulation with Applications, 3(2), 141-158.

Zhang, J., Li, S. (2022), Air quality index forecast in Beijing based on CNN-LSTM multi-model. Chemosphere, 308, 136180.